Synthesis and Characterization of Novel Mono and Di-Cationic Ionic Liquids for the Applications in Organic Transformations and Optoelectronics

A THESIS SYNOPSIS SUBMITTED TO

Institute of Advanced Research

For The Award of The Degree of

DOCTOR OF PHILOSOPHY

In

CHEMISTRY

Submitted By

Yash Bhagawatprasad Barot

(Reg. No. IAR/11572)

UNDER THE GUIDANCE OF

Supervisor

Dr. Roli Mishra

Associate Professor,

Department of Biotechnology and Bioengineering,

Institute of Advanced Research,

Gandhinagar, Gujrat, India

Co-Supervisor

Dr. Vivek Anand

Assistant Professor,

Department of Chemistry,

University Institute of Science,

Chandigarh University,

Mohali, Punjab**,** India

January-2024

TABLE OF CONTENT

	Page No.
Abstract	1
Chapter 1	
Introduction	2
Chapter 2	
Synthesis, Characterization and Physicochemical Properties of Novel Ionic Liquids	2
Chapter 3	
Application of Synthesized Imidazolium-based Di-cationic Ionic Liquids in Organic Transformation	5
Chapter 4	
Synthesis and Characterization of Conjugated Organic Molecules and Fluorescent Ionic Liquids	7
Chapter 5	
Application of the Synthesized Fluorescent ILs and Conjugated Organic Systems for Optoelectronics	9
Publications	18
Conferences	20

Abstracts

Ionic liquids have distinguished themselves as safer, more environmentally friendly alternatives to conventional chemicals as solvents, additives, and catalysts in organic transformations. The thesis was primarily organized into five chapters. In the first chapter, a review of the literature on mono and di-cationic ionic liquids is given, along with information on their applications in organic transformations as catalyst and optoelectronics applications like aggregation-induced emission (AIE), white light emission (WLE), and as heavy metal sensors conjunction with conjugated organic molecules (COMs). The second chapter discusses the design, synthesis, and thermal properties comparison of novel di-cationic imidazolium based ionic liquids and DABCO based mono and di-cationic ionic liquids. In the third chapter, we discussed the use of novel synthesized di-cationic imidazolium ionic liquids as catalyst in the oxidation of alcohols and acylation of alcohols, phenols and amines. The synthesis and characterization of COMs and ionic liquids conjugated with COMs are covered in the fourth chapter. The fifth chapter discusses the use of fluorescent ionic liquid and COMs in AIE, WLE, and sensing. Also, the mechanistic study of WLE, AIE and sensing was studied using the different techniques.

Chapter 1: Introduction

A brief literature review of mono and di-cationic ionic liquids, and the use of these ionic liquids as catalysts in organic transformation are covered in this chapter. Additionally, several literature research has demonstrated the significance of aggregation-induced emission, sensing, and white light generation in conjugated molecules and fluorescent ionic liquids for optoelectronic applications.

Objectives of the Present Work

1. Synthesis and Characterization of Imidazolium and DABCO based Mono and Di-cationic Ionic Liquids and Compare Their Physicochemical Properties
2. Investigation of Di-cationic Ionic Liquids Applications as Catalyst
3. Synthesis of Fluorescent Ionic Liquids (FILs) and Conjugated Organic Molecules (COMs)
4. Applications of COMs and FILs in Optoelectronics Applications like AIEE, WLE and Sensing

Chapter 2: Synthesis, Characterization and Physicochemical Properties of Novel Ionic Liquids

We have discussed the synthesis, characterization, and thermal properties of mono and dicationic ionic liquids based on imidazolium and DABCO in this chapter. Ionic liquids-based imidazolium and DABCO were synthesized as per Scheme 1.0 to 3.0.

Both the imidazolium-based dicationic ionic liquid $[DIL]^{2+}[Cr_2O_7]^{2-}$ and $[DIL]^{2+}[2FeCl_4]^{2-}$ were synthesized for the first time using the standard literature procedures. For the synthesis of $[DIL]^{2+}[Cr_2O_7]^{2-}$, at first N-methylimidazole **(1)** is initially treated with 1,2 dichloroethane **(2)** at 80 °C to give $[DIL]^{2+}[2Cl]^{2-}$ **(3) (Scheme 1)**. The resulting $[DIL]^{2+}[2Cl]^{2-}$ **(3)** was then used to produce $[DIL]^{2+}[2OH]^{2-}$ **(4)** through anion exchange with sodium hydroxide **(Scheme 1)**. $[DIL]^{2+}[2OH]^{2-}$ **(4)** and CrO_3 **(5)** were mixed in water to yield an identical amount of dichromate ionic liquid $[DIL]^{2+}[Cr_2O_7]^{2-}$ **(6) (Scheme 1)**. Furthermore, for the synthesis of $[DIL]^{2+}[2FeCl_4]^{2-}$, $[DIL]^{2+}[2Cl]^{2-}$ **(3)** was reacted with ferric chloride in methanol for 4 hrs at

room temperature yielded the desired $[DIL]^{2+}[2FeCl_4]^{2-}$ **(7) (Scheme 1)**. The structure of $[DIL]^{2+}[Cr_2O_7]^{2-}$ and $[DIL]^{2+}[2FeCl_4]^{2-}$ and all the intermediates ($[DIL]^{2+}[2Cl]^{2-}$ and $[DIL]^{2+}[2OH]^{2-}$) were characterized by spectroscopic tools.

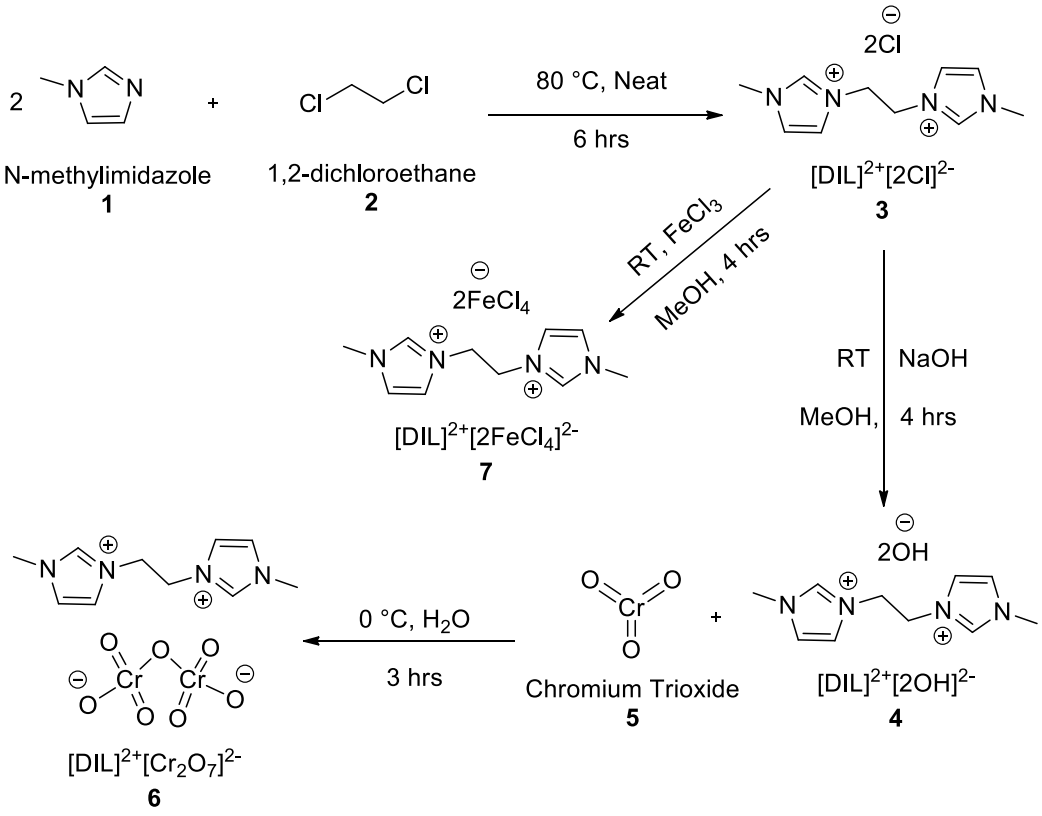

Scheme 1: Synthetic route followed for Imidazolium based DILs

For the synthesis of DABCO functionalized mono (MILs) and di-cationic ionic liquids (DILs), Firstly the MILs were synthesized by reacting DABCO **(8)** with an equal molar of 3-chloro-1-2-propane diol **(9)** to give $[DABCO\text{-}PDO]^{+}[Cl]^{-}$ **(10) (Scheme 2)**. Then, a solution of **(10)** in MeOH was added to the methanolic solution of NaOH and heated at 60 °C to give corresponding $[DABCO\text{-}PDO]^{+}[OH]^{-}$ **(11) (Scheme 2)**. Moreover, $[DABCO\text{-}PDO]^{+}[OH]^{-}$ **(11)** was reacted with proline **(12)** for 6 hrs at 60 °C to get $[DABCO\text{-}PDO]^{+}[Pro]^{-}$ **(13) (Scheme 2)**. On the other hand, for the synthesis of $[DABCO\text{-}PDO]^{+}[NTf_2]^{-}$ **(14),** $[DABCO\text{-}PDO]^{+}[Cl]^{-}$ **(10)** on reaction with aqueous solution of lithium triflimide at 60 °C for 6 hrs, yielded the desired $[DABCO\text{-}PDO]^{+}[NTf_2]^{-}$ **(14) (Scheme 2)**.

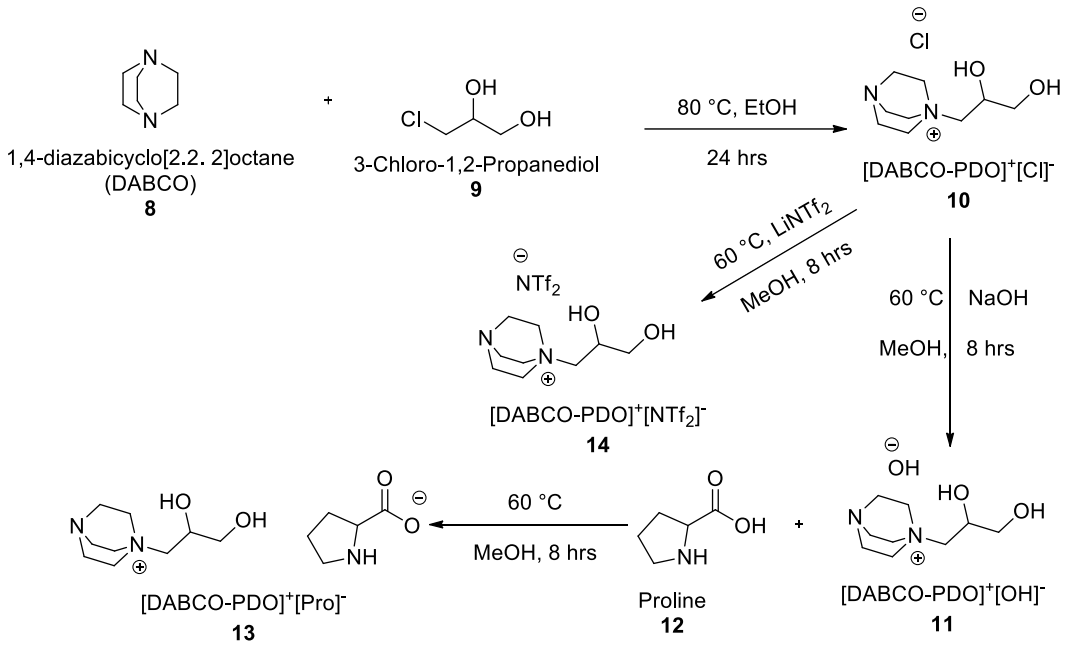

Scheme 2: Synthetic route followed for DABCO based MILs

The DILs $[DABCO\text{-}PDO]^{2+}[2Cl]^{2-}$ **(15),** $[DABCO\text{-}PDO]^{2+}[2OH]^{2-}$ **(16),** $[DABCO\text{-}PDO]^{2+}[2Pro]^{2-}$ **(17)** and $[DABCO\text{-}PDO]^{2+}[2NTf_2]^{2-}$ **(18)** were prepared using the same procedure as it was followed for the synthesis of MILs except the 2 equivalents of **(9)** and other anion exchange resins were used **(Scheme 3)**. All of the synthesized compounds were thoroughly characterized using various spectroscopic techniques.

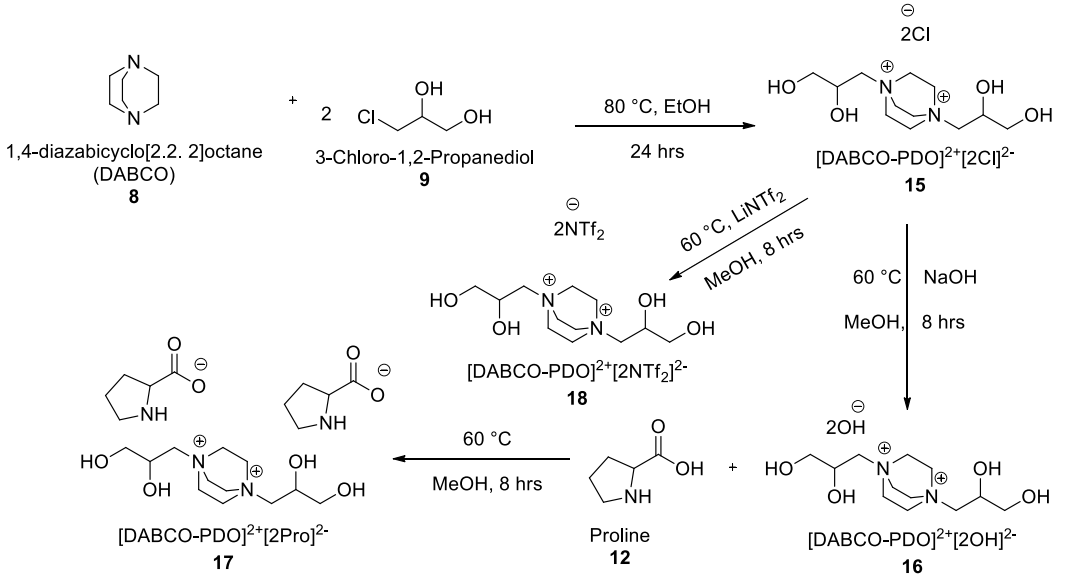

Scheme 3: Synthetic route followed for DABCO based DILs

The thermal properties of all MILs and DILs were examined using Thermogravimetric Analysis (TGA) and Differential Scanning Calorimetry (DSC) studies. These experiments were carried out at a 10 °C/min heating rate in an N_2 atmosphere. When comparing the decomposition temperatures of DABCO functionalized DILs and MILs with the same anions and cations, it was clear that the DILs have a range of 26-35 °C higher decomposition temperatures **(Table 1)**. We have also demonstrated the thermal stability of $[DIL]^{2+}[Cr_2O_7]^{2-}$ (T_{onset} 290 °C) and $[DIL]^{2+}[2FeCl_4]^{2-}$ (T_{onset} 310 °C). As expected, both the imidazolium-based DILs show higher thermal stability than the DABCO-functionalized DILs. The DILs are thus suitable for utilization at high-temperature conditions and applications related to local heating such as lubrication rather than the corresponding MILs.

Table 1: Thermophysical properties of the MILs and DILs

Thermal Properties	T^{decom}/°C[a]	M.p. /°C[b]	T_g^{onset}/°C[c]
$[DIL]^{2+}[Cr_2O_7]^{2-}$	290 °C	123.7 °C	-39.0 °C
$[DIL]^{2+}[2FeCl_4]^{2-}$	310 °C	80 °C	-48.6 °C
$[DABCO\text{-}PDO]^{+}[OH]^{-}$	237 °C	97 °C	-30.3 °C
$[DABCO\text{-}PDO]^{+}[Pro]^{-}$	183 °C	80 °C	-19.27 °C
$[DABCO\text{-}PDO]^{+}[NTf_2]^{-}$	261 °C	73 °C	ND
$[DABCO\text{-}PDO]^{2+}[2OH]^{2-}$	266 °C	115 °C	-43.9 °C
$[DABCO\text{-}PDO]^{2+}[2Pro]^{2-}$	217 °C	116.8 °C	-30.62 °C
$[DABCO\text{-}PDO]^{2+}[2NTf_2]^{2-}$	287 °C	89 °C	ND

According to the information in **Table 1**, all MILs and DILs are true room temperature ionic liquids with the exception of $DIL]^{2+}[Cr_2O_7]^{2-}$, $[DABCO\text{-}PDO]^{2+}[2OH]^{2-}$ and $[DABCO\text{-}PDO]^{2+}[2Pro]^{2-}$ which have higher melting points than 100 °C. In terms of the cation effect, it is evident that the DILs melting points are significantly greater than those of the MILs. One of the key elements that were discovered to influence the melting points of the various MILs and DILs is the nature of the anion.

Chapter 3: Application of Synthesized Imidazolium-based Di-cationic ILs in Organic Transformation

Here, we describe the application of $[DIL]^{2+}[Cr_2O_7]^{2-}$ for converting primary aromatic alcohols and their derivatives into aldehyde and $[DIL]^{2+}[2FeCl_4]^{2-}$

as catalyst for converting alcohols, phenols and amines into acetate. The developed methods have several advantages, including rapid reaction time, recyclability of the catalyst, and easy recovery of the catalyst after each cycle (without any workup). These results offer a wide opportunity to use these catalysts in organic transformations.

To standardize the oxidation reaction conditions, a number of studies were conducted to study the effects of solvents, mol% of ionic liquid, temperature, and different substrate types. As shown in **Table 2**, entries 1-8, 11 and 16, an electron-donating group at the aromatic nucleus accelerated the reaction and produced high yields of the corresponding carbonyl products. In contrast, an electron-withdrawing group at the aromatic nucleus slowed down the reactions and produced relatively lower yields of carbonyl products (Table 1, entries 9, 10, 12, 13). By using ^{1}H NMR and ^{13}C NMR spectroscopy, the structures of the produced products were verified.

Table 2: Oxidation of alcohols, in the presence of $[DIL]^{2+}[Cr_2O_7]^{2-}$

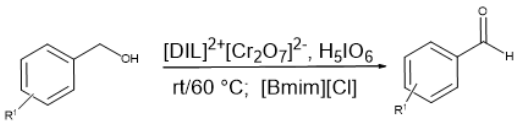

Entry	Substrate (R^1)	Product	Yield[a,b] (%) r.t	Yield[a,b] (%) 60 °C
1	4-OCH_3	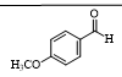	90% (60 min)	94% (10 min)
2	3-OCH_3	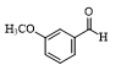	92% (50 min)	93% (10 min)
3	3,4-OCH_3	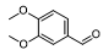	93% (40 min)	95% (10 min)
4	3,4,5-OCH_3	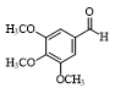	90% (40 min)	91% (07 min)
5	4-OH,3-OMe	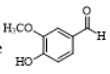	91% (50 min)	93% (15 min)
6	4-OH	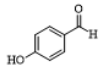	90% (30 min)	88% (05 min)
7	2-OH		92% (30 min)	93% (05 min)
8	3,4-OH	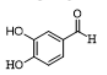	86% (40 min)	90% (10 min)
9	3-NO_2	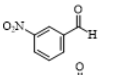	88% (180 min)	91% (40 min)
10	4-NO_2	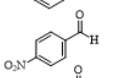	84% (190 min)	89% (50 min)
11	4-Cl	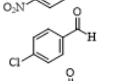	90% (45 min)	91% (10 min)
12	2-Cl		91% (45 min)	91% (10 min)
13	4-CH_3	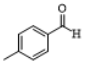	94% (45 min)	94% (07 min)
14	(1H-Indol-3-yl)-methanol		92% (40 min)	94% (08 min)
15	Cyclohexyl-methanol		93% (40 min)	94% (07 min)
16	Pyridin-3-yl methanol		92% (40 min)	94% (07 min)

We also pay attention to the reusability of ionic liquid; $[DIL]^{2+}[Cr_2O_7]^{2-}$ was reusable four times in a shorter period of time than it was in the fifth cycle, during which the reaction took longer time and the catalyst produced less yield of the substrate. In the presence of periodic acid, $[DIL]^{2+}[Cr_2O_7]^{2-}$, and 4-

methoxy benzyl alcohol, a model substrate for the oxidation reaction, we hypothesized a mechanism **(Scheme 4)**.

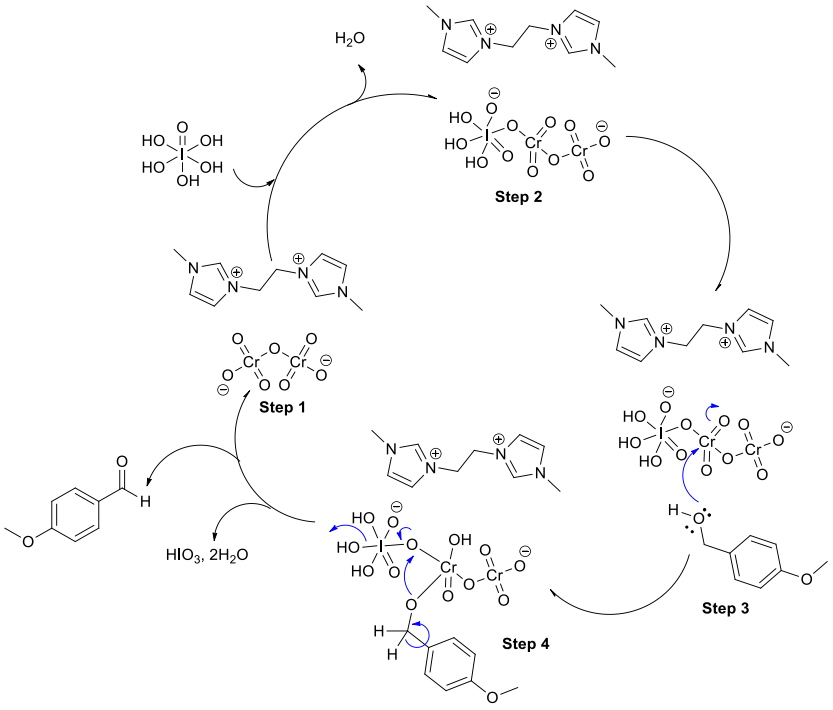

Scheme 4: Plausible reaction mechanism for the oxidation of alcohols using catalyst system $[DIL]^{2+}[Cr_2O_7]^{2-}/H_5IO_6$

Chapter 4: Synthesis and Characterization of Conjugated Organic Molecules and Fluorescent Ionic Liquids

In this chapter, we have discussed the synthesis of three new fluorescent ionic liquids (FILs) named [TPA-SB][Br], [PTZ-SB][Br] and RhB-IL and two new conjugated organic molecules (COMs) called DTPA-SB and DPTZ-SB. The FILs and COMs were characterized in detail using spectroscopic tools and their photophysical properties were studied by UV–visible/fluorescence spectroscopy. All of the compound syntheses were carried out in the manner depicted in Schemes 5 to 7.

For the synthesis of triphenylamine-based Schiff base DTPA-SB, at first triphenylamine **was** formylated to give triphenylamine aldehyde, TPA-CHO. Then, was reacted with ethylenediamine in methanol under refluxing conditions for 12 hours to give the required moiety DTPA-SB **(Scheme 5)**. For the synthesis of fluorescent ionic liquid (FIL), firstly the IL was synthesized by reacting 1-methylimidazole with 2-bromoethylamine to give

[2-aemim][Br]. Then, the Schiff base [TPA-SB][Br] was obtained on reacting TPA-CHO with [2-aemim][Br] in CH_3OH at a temperature of 65 °C for 6 hours **(Scheme 5)**.

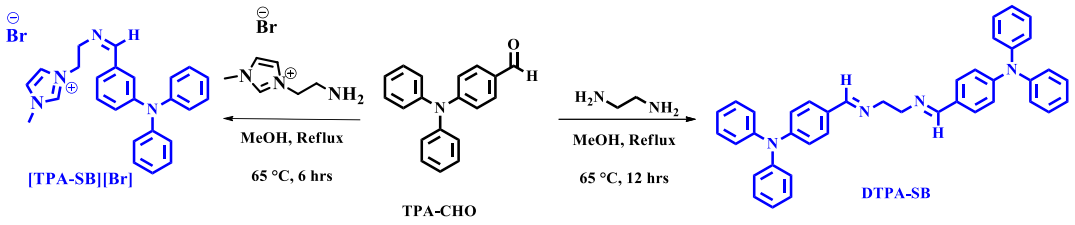

Scheme 5: Synthesis of DTPA-SB and [TPA-SB][Br]

On the other hand, for the synthesis of phenothiazine-based Schiff base DPTZ-SB, first phenothiazine was alkylated with hexyl bromide to give hexylphenothiazine**,** which on formylation resulted in the formation of hexylphenothiazine aldehyde, PTZ-CHO **(Scheme 6)**. Then PTZ-CHO on reaction with ethylenediamine in methanol under refluxing conditions for 12 hrs, yielded the desired DPTZ-SB **(Scheme 6)**. For the synthesis of phenothiazine-based ionic liquid Schiff base [PTZ-SB][Br], PTZ-CHO on reaction with [2-aemim][Br] in methanol at reflux for 6 hrs, yielded the desired [PTZ-SB][Br] **(Scheme 6).**

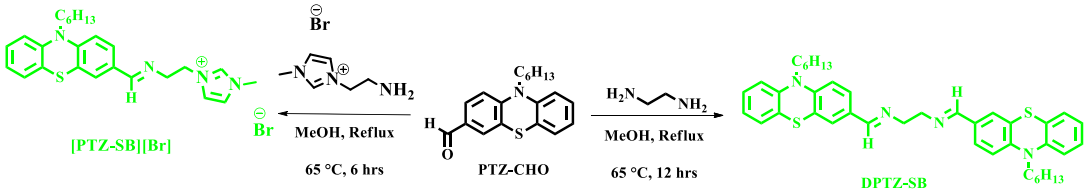

Scheme 6: Synthesis of DPTZ-SB and [PTZ-SB][Br]

Moreover, for the synthesis of FIL, first Rhodamine B base was first treated with $SOCl_2$ to produce rhodamine acid chloride. Then, it was subjected to a 24-hour reflux reaction with 1-methylimidazole to produce RhB-IL, as a red viscous liquid **(Scheme 7)**.

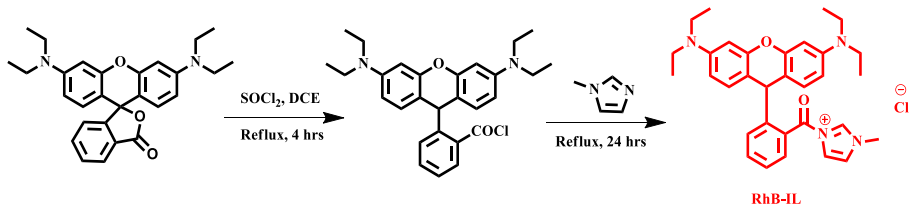

`**Scheme 7:** Synthesis of RhB-IL

Chapter 5: Application of the Synthesized Fluorescent ILs and Conjugated Organic Systems for Optoelectronics

We have successfully synthesized and characterized five new fluorophores as discussed in the previous chapter. Now their application in optoelectronics like AIEE, WLE and sensing are discussed here.

Aggregation Induced Enhanced Emission (AIEE)

The COMs (DTPA-SB, DPTZ-SB) and FILs ([TPA-SB-Br], [PTZ-SB][Br], and RhB-IL) were studied for AIEE in a THF-water mixture with 0 to 99% water fractions, at a constant concentration of 10^{-5} M for each measurement. The emission and absorption spectra of [PTZ-SB][Br] under various water fractions (*fw*) are shown in **Figures 1(a) and 1(b)**, respectively.

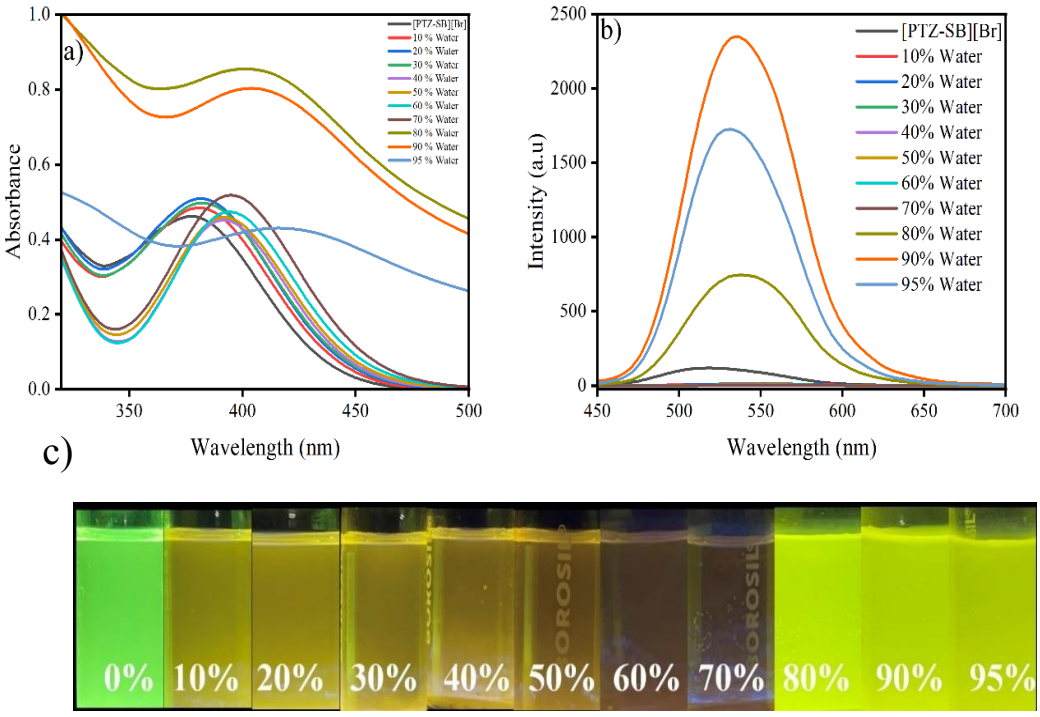

Figure 1: a) UV-visible spectra of [PTZ-SB][Br] (1×10^{-5} M) in solution state for different water-THF fractions. b) PL spectra of [PTZ-SB][Br] (1×10^{-5} M) in solution state for different water-THF fractions and c) Photographs of the solutions of [PTZ-SB][Br] (1×10^{-5} M) in different THF-water fractions (0% to 95%)

The λ_{max} absorbance for pure THF was noted at 378 nm, as can be shown in **Figure 1(a)**. The emission spectra of [PTZ-SB][Br] demonstrated a maximum

emission at 520 nm in pure THF. An increase in fluorescence intensity was noted when the water fraction (*fw*) was increased. Surprisingly, the highest increase was seen at 90% *fw*, with a redshift of 15 nm and a rise in intensity of 38.1 times as compared to that for pure THF. Indeed, in the process, the color change observed was from green (for 0 % *fw*) to yellow (for 90 % water fraction) **[Figure 1(c)].** Dynamic light scattering (DLS) investigations were carried out to explore deeper into the AIEE behavior of [PTZ-SB][Br]. The results show that the [PTZ-SB][Br] particles had an average diameter of 721.4 nm in pure THF. On the other hand, the particle size decreased to 270.9 nm for 80% water. In addition, the size for 90% water was further decreased to 161.2 nm.

Similar trends were seen in the AIEE investigations for various compounds, including DTPA-SB, DPTZ-SB, [TPA-SB][Br], and RhB-IL. In comparison to pristine THF solution, the emission intensities of DTPA-SB, DPTZ-SB, [TPA-SB][Br], and RhB-IL increased 7.6, 9.4, 31.2, and 7.7 folds, with a redshifts of 24, 25, 11, and 4 nm, respectively.

Sensing Abilities of COMs and FILs

Selectivity experiments of the COMs and FILs were conducted in order to investigate their sensing capabilities towards metal cations. Twelve heavy metal ions were chosen to study selectivity. The concentrations of the metal ions were set at 1×10^{-3} M in H_2O and that of [PTZ-SB][Br] was 1×10^{-5} M in THF. **Figure 2(a)** shows that there were slight variations in the fluorescence intensity of [PTZ-SB][Br] with the addition of the ions Cu^{2+}, $Ni^{2+,}$ Pb^{2+}, Co^{2+}, Hg^{2+}, Fe^{2+}, Zn^{2+}, Sn^{2+}, Mn^{2+}, Ag^{1+} and Fe^{3+} ions. However, only the addition of the Cd^{2+} ion resulted in a considerable fluorescence quenching of [PTZ-SB][Br] solution. The green fluorescence was entirely quenched upon the addition of Cd^{2+} ion, as seen in the inset of **Figure 2(b)**. Similar investigations on selectivity were conducted on DTPA-SB, DPTZ-SB, [TPA-SB][Br], and RhB-IL. The presence of Cu^{2+}, Fe^{3+} ions, and 30 % H_2O_2 suppressed the emission intensities of DTPA-SB. The emission intensity of the DPTZ-SB, [TPA-SB][Br], and RhB-IL was reduced in the presence of Picric Acid (PA), Sn^{2+} and Hg^{2+}, respectively.

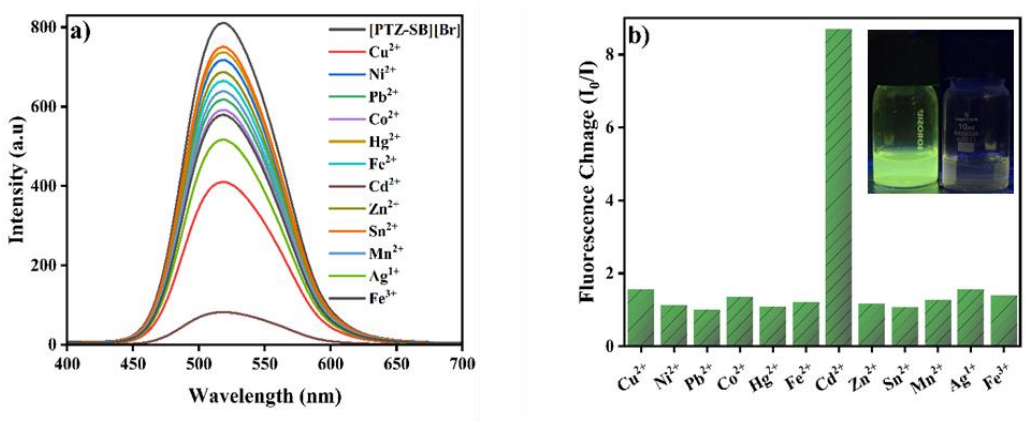

Figure 2 a) Fluorescence spectra of [PTZ-SB][Br] (1×10^{-5} M) in presence of twelve metal cations (1×10^{-3} M) in THF-H_2O mixtures b) The emission quenching efficiency (I_0/I) of [PTZ-SB][Br] (1×10^{-5} M) in presence of twelve heavy metal ions (1×10^{-3} M) . Inset of b) shows the fluorescence image of [PTZ-SB][Br] in absence and presence of Cd^{2+}metal ion (left to right) in THF-water mixture under UV-light

Another factor to consider while assessing the effectiveness of a sensor is its sensitivity towards metal cation. PL titrations were carried out for the successive addition of 30 µL each of Cd^{2+} (10^{-4} M in H_2O) to a 10^{-5} M solution of the [PTZ-SB][Br] in THF in order to complete the sensitivity studies. **Figure 2(a)** shows that as the amount of Cd^{2+} ions increased, the emission intensity of [PTZ-SB][Br] gradually decreased until the quenching reached saturation (for 240 µL of Cd^{2+}).

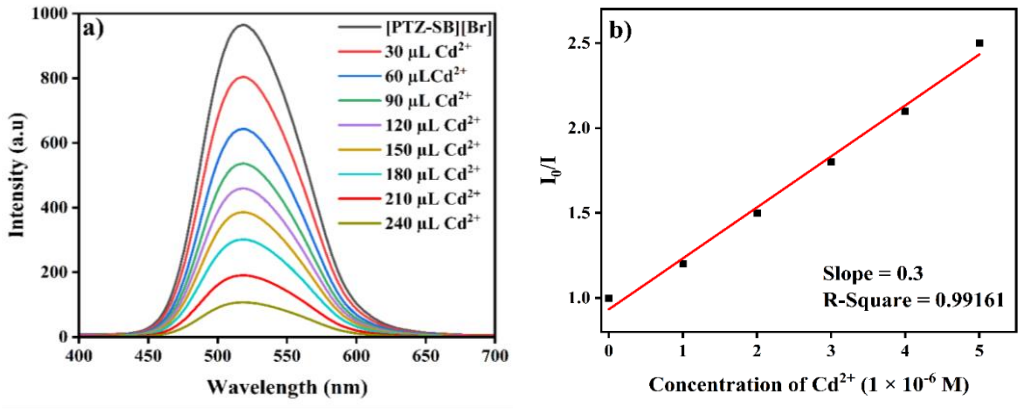

Figure 2 a) Change in the emission spectra of [PTZ-SB][Br] (1×10^{-4} M in THF) with the gradual addition of different concentrations of Cd^{2+} (1×10^{-4} M

in water) ions and b) Stern-Volmer plot of [PTZ-SB][Br] in presence of different concentrations of Cd^{2+} ions

Investigating the limit of detection (LOD) and binding constant was done using the titration curve. The Stern-Volmer plot shown in **Figure 2(b)**, compares the relative change in [PTZ-SB][Br] fluorescence intensity upon the addition of different concentrations of Cd^{2+} ions. As a result, the K_a and LOD for Cd^{2+} ions were determined to be 5.44×10^8 M^{-1} and 3.8×10^{-7} M, respectively. Similar studies were carried out for different metal ions using DTPA-SB, DPTZ-SB, [TPA-SB][Br] and RhB-IL which show lower LOD and higher binding constant as shown in **Table 3**.

Table 3: LOD and K_a of different analytes using COMs and FILs

Molecules	Metals	LOD	K_a (M^{-1})	Stoichiometric Ratio (Metal:Ligand)
COMs				
DTPA-SB	Cu^{2+}	1.06 nM	6.54×10^{10}	2:1
	Fe^{3+}	2.4 nM	5.5×10^{10}	2:1
	30 % H_2O_2	0.19 µM	9.90×10^9	2:1
DPTZ-SB	PA	0.8 nM	4.05×10^{10}	2:1
FILs				
[TPA-SB][Br]	Sn^{2+}	0.69 µM	3.1×10^{10}	1:2
RhB-IL	Hg^{2+}	0.25 µM	5.01×10^7	1:1

Paper-based Fluorescent Sensor

To date, heavy metal sensing detection approaches typically require intricate operating processes and expensive devices. As a result, a quick and easy technique of detection is necessary. With these facts in mind, an easy-to-use, portable, and cost-effective paper-based fluorescence sensor immobilized with COMs and FILs has been developed for the quick monitoring of various heavy metal ions, explosives, and peroxide.

Figure 3(a) depicts the variations in the PL spectrum caused by the progressive addition of various concentrations of Cd^{2+}. On the steady addition of Cd^{2+}, it is evident that the fluorescence intensity of the paper-based sensor subsequently decreases. The minimum concentration at which Cd^{2+} is visible to the unaided eye is 2 nM. The paper-based sensor was further used to detect solid traces of Cd^{2+}. In this experiment, Cd^{2+} solid residue was ground into a

powder and sprinkled over the surface of fluorescent paper. The PL quenching process was then observed under the UV light illumination, as shown in **Figure 3(c).** According to the sensing studies conducted in a suspension medium, the Stern-Volmer and modified Stern-Volmer plots were used to assess the LOD and binding constant for the paper-sensor towards Cd^{2+}. The LOD is 0.16 nM **[Figure 3(b)]** and the binding constant is 1.8×10^{10} M^{-1}.

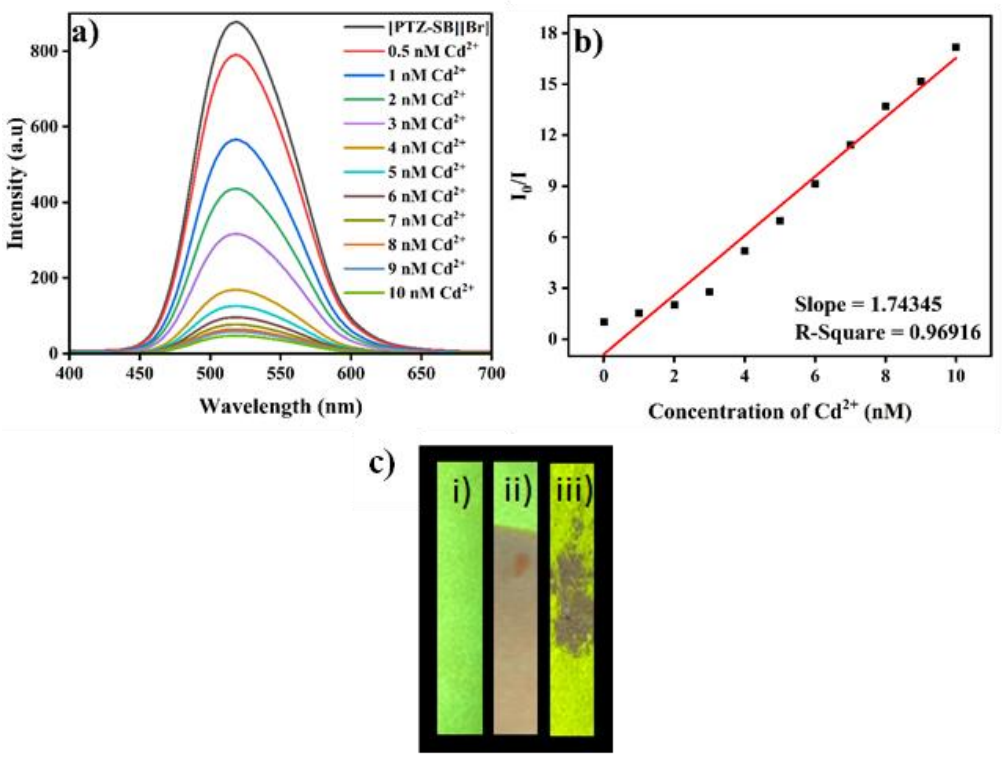

Figure 3: a) Fluorescence quenching spectra of paper sensor based on [PTZ-SB][Br] on addition of various concentrations of Cd^{2+}. b) Stern–Volmer plot of paper-based sensor in the presence of different concentrations of Cd^{2+} ions (in the nM range). and c) Photographs of paper-sensor under UV light illumination for i) [PTZ-SB][Br] alone, ii) 10 nM solution of Cd^{2+} with [PTZ-SB][Br] and iii) Cd^{2+} powder with [PTZ-SB][Br]

A color-scanning mobile app was incorporated, which scanned the green (G) and red (R) color intensities of the picture, in order to test the on-site detection capability of the paper-based sensor. For this, a smartphone was used to capture a PL color image of the paper-based device at various Cd^{2+} concentrations, and an app was then used to determine R/G ratios for each concentration. **Figure 4** depicts a calibration curve that was plotted for the

various Cd^{2+} concentrations based on R/G ratio values. **Table 4** illustrate the LOD, K_a and recycling times of different paper sensor fabricated using COMs and FILs for sensing different analytes.

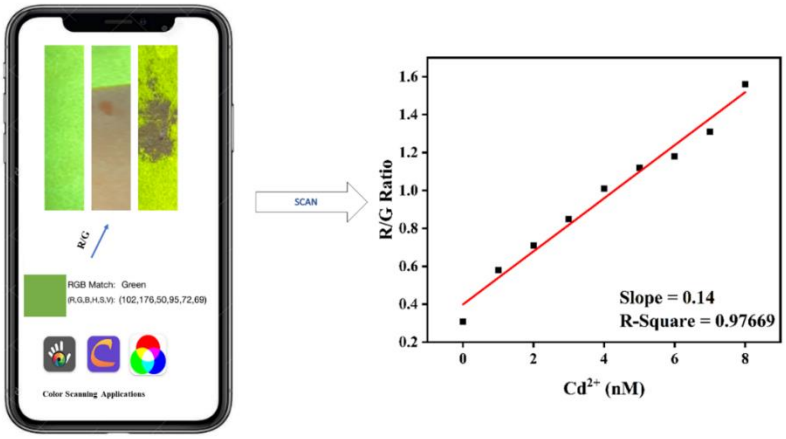

Figure 4: Calibration graph for the paper-based sensor in collaboration with a smartphone App for Cd^{2+} detection

Table 4: LOD, K_a, and recycling of paper sensor of COMs and FILs for detection of different analytes

Molecules	Metals	LOD	K_a (M^{-1})	Recycle
		COMs		
DTPA-SB	30 % H_2O_2	2.3 nM	1.67×10^{11}	4
DPTZ-SB	PA	0.17 nM	1.5×10^{10}	13
		FILs		
[TPA-SB][Br]	Sn^{2+}	2.1 nM	1.57×10^{10}	6
RhB-IL	Hg^{2+}	0.21 nM	1.61×10^{11}	4

Mechanistic Study of COMs and FILs for Sensing

A ^1H NMR titration experiment was performed in DMSO-d_6 as shown in **Figure 5** to better understand the binding sites accessible on [PTZ-SB][Br] for its interaction with Cd^{2+} ions. The signal of the -CH proton accessible at the C2 location in imidazole was gradually pushed downfield from 9.7 ppm to 10.3 ppm with the addition of 1.0 equivalent of nitrate salt of Cd^{2+} (According to Job's plot). Another notable alteration in the spectra was the displacement of the proton signal of the HC=N found in [PTZ-SB][Br] downfield from 8.25 ppm to 8.40 ppm. Proton signals between 7.10 and 7.97 ppm changed downfield to 7.18 and 8.15 ppm, while the 4.63 ppm -NCH2 proton signal

dramatically moved up-field to 4.28 ppm. These findings clearly imply that HC=N and the imidazolium group are involved in the chelation process that culminates in the development of the Cd-L (ligand) complex.

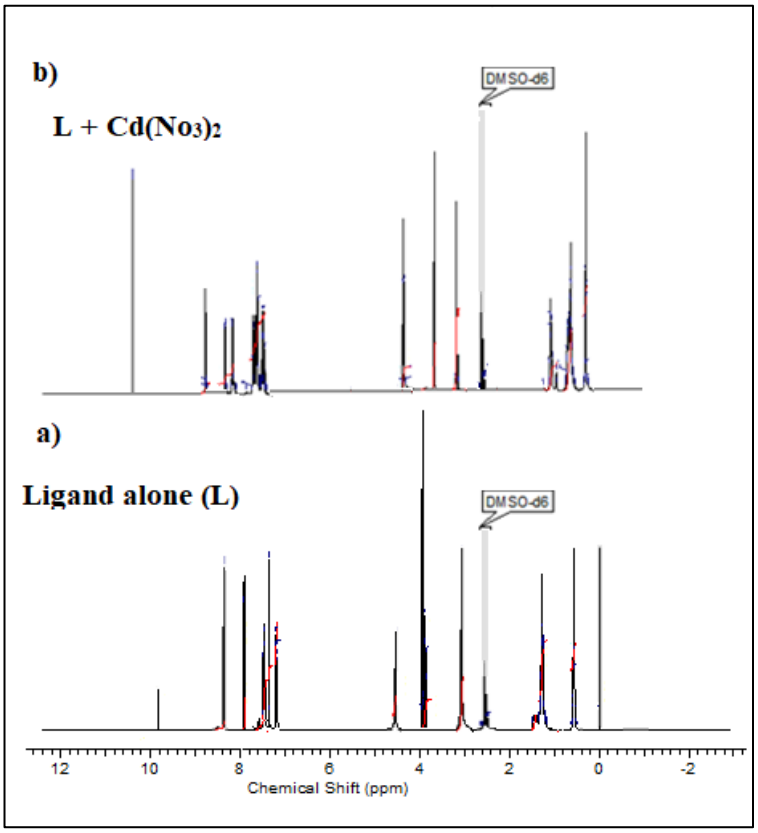

Figure 5: a) ^{1}H NMR spectra of [PTZ-SB][Br] (in DMSO-d_6) alone and b) ^{1}H NMR spectra of [PTZ-SB][Br] in presence of 1.0 equivalent of nitrate salt of Cd^{2+} ions (in DMSO-d_6)

White Light Emission (WLE)

In the current work, blue, green, and red emitting organic compounds based on **Systems I** (DTPA-SB, DPTZ-SB, and Rh-B) and **Systems II** ([TPA-SB][Br], [PTZ-SB][Br], and RhB-IL) were combined to produce WLE **(Scheme 8)**. In a THF solution with a concentration of 10^{-5} M, the emission and absorption spectra of each emitter were recorded. **Figure 6(a-d)** shows the UV-visible, fluorescence, and CIE (Commission Internationale d'Eclairage) chromaticity diagrams for the THF-solubilized solutions of [TPA-SB][Br], [PTZ-SB][Br], and RhB-IL.

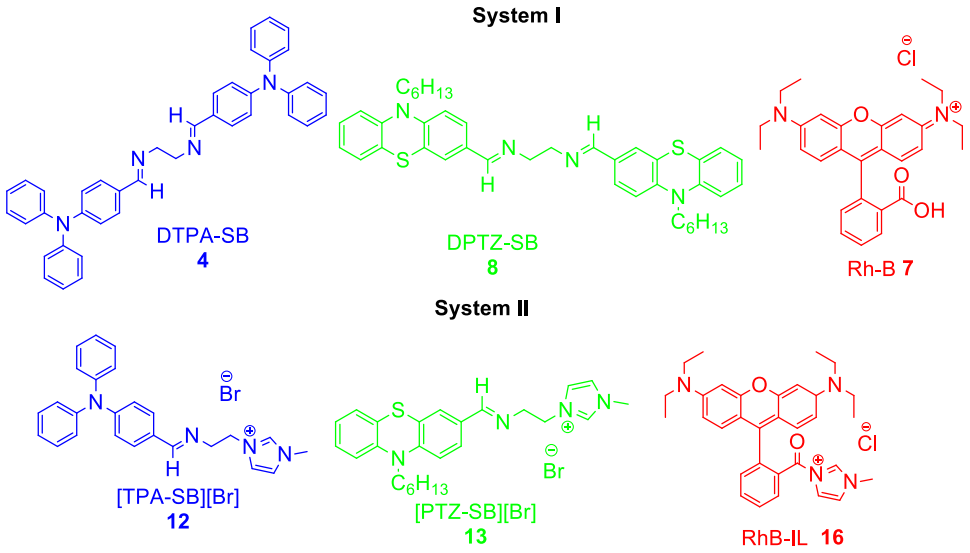

Scheme 8: Molecular structure of COMs and FILs utilized for WLE

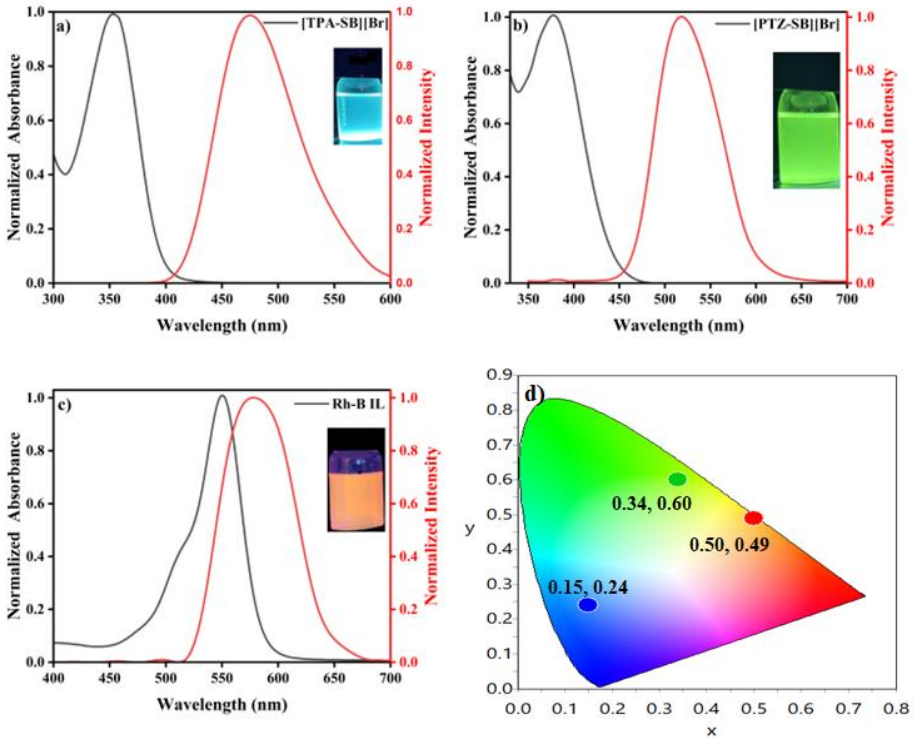

Figure 6 Normalized absorption and emission spectra for a) [TPA-SB][Br], b) [PTZ-SB][Br], c) RhB-IL in THF and d) the CIE coordinates of the corresponding [TPA-SB][Br] (Blue dot), [PTZ-SB][Br] (Green dot) and RhB-IL (Red dot) . The fluorescence colour of each chemical when exposed to UV light is shown in the inset of (a-c)

Table 5 includes the distinct photoluminescence properties of **System I** and **System II**. **Figure 7(a)** illustrates the emission spectra of System **II** with a

combination of 1 mL of [TPA-SB][Br] and [PTZ-SB][Br] and 1.4 mL of RhB-IL (10^{-4} M in THF) after photoexcitation at a wavelength of 354 nm, which showed two peaks with λ_{max}^{em} at 499 and 606 nm. Furthermore, the spectra acquired by the CIE had coordinates of x = 0.33 and y = 0.33, which are a perfect match with the typical CIE values for WLE.

Table 5: Photoluminescence properties of **System I** and **System II**

Compound	Absorbance (λ_{max}^{abs})	Emission (λ_{max}^{ems})	Fluorescence quantum yield	CIE coordinates
		System I		
DTPA-SB	345 nm	449 nm	0.13	(0.14,0.09)
DPTZ-SB	367 nm	509 nm	0.27	(0.22,0.56)
Rh-B	554 nm	580 nm	0.31	(0.50,0.47)
		System II		
[TPA-SB][Br]	354 nm	475 nm	0.18	(0.15,0.24)
[PTZ-SB][Br]	377 nm	518 nm	0.31	(0.34,0.60)
RhB-IL	550 nm	579 nm	0.30	(0.50,0.49)

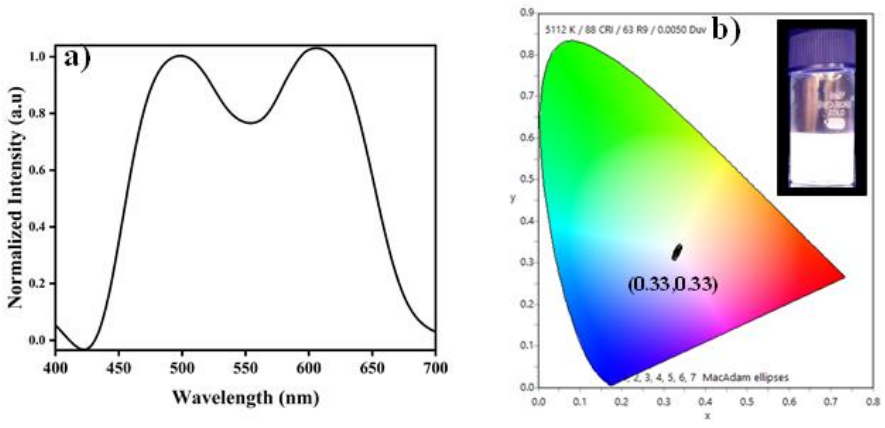

Figure 7: a) PL spectra of mixture of [TPA-SB][Br]:[PTZ-SB][Br]:RhB-IL in THF solution, excited at 354 nm and b) the CIE coordinates of the corresponding WLE. The photo of the white light taken under UV light irradiation is shown in the inset

List of Publications

Research Articles

1. **Yash B. Barot**, Vivek Anand and Roli Mishra. "Red-Emitting AIEE Active Rhodamine-based Ionic Liquid for the Ultrasensitive and Selective Detection of Mercury Ions" *ACS The Journal of Physical Chemistry B*, 127, 49, (2023) 10529-10541. https://doi.org/10.1021/acs.jpcb.3c05157 **(*IF=3.3*)**
2. **Yash B. Barot**, Vivek Anand and Roli Mishra. "White Light Emission from Fluorescent Ionic Liquids in the Solution and Gel forms using RGB system" *Journal of Photochemistry and Photobiology A: Chemistry*, 446,1, (2024):115109. https://doi.org/10.1016/j.jphotochem.2023.115109 **(*IF=4.3*)**
3. Sahil, Suresh Kumar**, Yash B. Barot**, Roli Mishra, Dilbag Singh and Neeraj Gupta. "Nitrogen-doped fluorescent active fullerenes as a fluorescent probe for the detection of Hg^{2+} ions in aqueous solutions" *Environmental Nanotechnology, Monitoring & Management* 20 (2023) 100845. https://doi.org/10.1016/j.enmm.2023.100845 **(Published)**
4. **Yash B. Barot**, Satyendra Mishra, Vivek Anand and Roli Mishra. "Iron Containing Di-cationic Ionic Liquid $[DIL]^{2+}[2FeCl_4]^{2-}$ as a Highly Efficient Catalyst for the Acylation of Alcohols, Phenols and Amines" *Catalysis Communication 182* (2023) 106739 https://doi.org/10.1016/j.catcom.2023.106739 **(*IF=3.7*)**
5. **Yash B. Barot**, Vivek Anand, Saurabh Vyas and Roli Mishra. "AIEE active ionic liquid based on triphenyl amine functionalized Schiff base for the selective and sensitive detection of Sn^{2+} ion." *Journal of Molecular Liquids* 382 (2023) 121875. https://doi.org/10.1016/j.molliq.2023.121875 **(*IF = 6.6*)**
6. **Yash B. Barot,** Vivek Anand, Saurabh Vyas and Roli Mishra. "Paper-based Device for Nanomolar Detection of Cd^{2+} Using AIEE-Active Imidazolium Ionic Liquid Functionalized Phenothiazine based Schiff-Base." *Journal of Molecular Liquids* 376 (2023) 121490. https://doi.org/10.1016/j.molliq.2023.121490 **(*IF = 6.6*)**

7. **Yash B. Barot**, Vivek Anand, and Roli Mishra. 2022a. "Aie-Active Phenothiazine Based Schiff-Base for the Selective Sensing of the Explosive Picric Acid in Real Water Samples and Paper-Based Device." *Journal of Photochemistry and Photobiology A: Chemistry* 434 (2022): 114224. **(*IF = 5.1*)**
8. **Yash B. Barot**, Vivek Anand, and Roli Mishra. 2022. "Phenothiazine and Triphenylamine-Based Fluorescent Schiff Bases for the Dual Application of White Light Generation and H_2O_2 Sensing." *New Journal of Chemistry* 46: (2022): 15666–77. **(*IF = 3.9*)**
9. **Yash B. Barot,** Vivek Anand, and Roli Mishra. 2022. "Di-Triphenylamine-Based AIE Active Schiff Base for Highly Sensitive and Selective Fluorescence Sensing of Cu^{2+} and Fe^{3+}." *Journal of Photochemistry and Photobiology A: Chemistry* 426 (2021): 113785. **(*IF = 5.1*)**
10. Kailash Devi, Vivek Anand, **Yash B. Barot**, Roli Mishra, Prashant Kumar, Vishal Mutreja. "Natural Pigments-Based Two Component White Light Emitting Systems" *Journal of Fluorescence* **(Under Review, Research Article)**

Review Articles

1. Vivek Anand, Roli Mishra, and **Yash Barot**. "Recent Advances in the Development of Pure Organic White Light Emitters." *Dyes and Pigments* (2021): 109390. **(Published, *IF = 5.1*)**

Book Chapters

1. Roli Mishra, Satyendra Mishra, Snehkrishn A. Chaubey, and **Yash B. Barot**. "Ionic liquids as alternative greener solvents and catalysts." *Handbook of Greener Synthesis of Nanomaterials and Compounds: Volume 1: Fundamental Principles and Methods* (2021): 359. **(Published)**

2. Roli Mishra, Satyendra Mishra, and **Yash B. Barot**. "Greener synthesis and stabilization of metallic nanoparticles in ionic liquids." In *Handbook of*

Greener Synthesis of Nanomaterials and Compounds, pp. 245-276. Elsevier, 2021. **(Published)**

Conference Attended

1. **Yash B. Barot**, Saurabh Vyas, Vivek Anand and Roli Mishra **(2022).** Insight on AIEE Properties of Phenothiazine based Ionic Liquid and Conjugated Organic Molecule: A Comparative Study. 22-23rd November 2022. GUJCOST sponsored **International conference** on "Recent Progresses in Chemical Sciences" organized by M.N Collage, Visnagar **(Poster, Awarded 2nd Prize)**
2. **Yash B. Barot**, Vivek Anand and Roli Mishra **(2021).** Synthesis of Phenothiazine and Triphenylamine based Schiff Bases for Aggregation Induced Enhanced Emission: "United We Stand, Divided We Fall". 29th-30th November 2021. Annuanl Research & Innovation Conclave (ARIC)-2021 organized by IAR, Gandhinagar **(Poster)**

Workshop/ Training

1. 7-Day Workshop on "STUTI-ANALYTICAL SCANNING ELECTRON MICROSCOPY**"** held from 25th April - 1st May, 2022 funded by the Department of Science & Technology (DST) at IIT, Gandhinagar
2. 7-Day Workshop on "FLUORESCENCE BASED CHARACTERIZATION TECHNIQUES**"** held from 4th-10th July, 2022 funded by the Department of Science & Technology (DST) at IAR, Gandhinagar
3. 2-Day Workshop on "Hands-on Training on Chromatography and Spectroscopy Techniques in Chemistry**"** held from 8th - 9th July, 2022 organized by Department of Biotechnology and Bioengineering at IAR, Gandhinagar
4. 5-day Workshop on "Intellectual Property Rights and Innovations" held from 8th-13th December, 2022 organized IAR, Gandhinagar
5. 5-day Workshop on "Outcome based Teaching-Learning Practices and Research" held from 13th-19th June, 2023 organized by IAR, Gandhinagar

Manuscripts Under Preparation

1. **Yash B. Barot**, Vivek Anand, Satyendra Mishra and Roli Mishra. "Chromium Functionalized, Imidazolium Di-Cationic Ionic Liquid: Highly Efficient Catalyst System for the Oxidation of Aromatic Primary Alcohols." **(Research Article)**
2. **Yash B. Barot**, Vivek Anand, Satyendra Mishra and Roli Mishra. "Novel DABCO based Mono-Cationic and Di-Cationic Ionic Liquids: A Comparative Study of Thermophysical Properties" (**Research Article)**
3. Kailash Devi, Prashant Kumar, **Yash B. Barot**, Roli Mishra, Vishal Mutreja and Vivek Anand. "Recent Advances in the Development of Pure Organic Mechanochromic Materials Composed of Potential Organic Fluorophores." (**Review Article)**